Applied Mathematical Modelling 68 (2019) 169–181

Contents lists available at ScienceDirect

Applied Mathematical Modelling

journal homepage: www.elsevier.com/locate/apm

Stepwise covariance matrix decomposition for efficient simulation of multivariate large-scale three-dimensional random fields

Dian-Qing Li[a,*], Te Xiao[a], Li-Min Zhang[b], Zi-Jun Cao[a]

[a] State Key Laboratory of Water Resources and Hydropower Engineering Science, Institute of Engineering Risk and Disaster Prevention, Wuhan University, 299 Bayi Road, Wuhan 430072, PR China

[b] Department of Civil and Environmental Engineering, The Hong Kong University of Science and Technology, Clear Water Bay, Kowloon, Hong Kong

ARTICLE INFO

Article history:
Received 22 June 2018
Revised 26 October 2018
Accepted 1 November 2018
Available online 13 November 2018

Keywords:
Spatial variability
Random field
Separable correlation function
Large-scale simulation
Site characterization
Reliability analysis

ABSTRACT

The spatial variability of geomaterials affects the failure mechanism and reliability of geotechnical structures significantly, and can be modeled rigorously as a three-dimensional (3-D) random field. However, the simulation of multivariate, large-scale and high-resolution 3-D random fields is a challenging task due to extraordinary demands in computational resources. This paper proposes a stepwise covariance matrix decomposition method (CMD) with the aid of separable correlation functions, in which the 3-D random field is generated sequentially along each single dimension with small one-dimensional correlation matrices. The method not only inherits the simplicity of the widely-used general CMD, but also significantly reduces the computational time and required memory space. It only takes a few seconds to construct large-scale and high-resolution 3-D random fields, with the requirement on memory space reduced by more than ten orders of magnitude. The maximum random field resolution is significantly improved from approximately $21 \times 21 \times 41$ using the general CMD to over $501 \times 501 \times 1001$ using the stepwise CMD, which suffices in most engineering applications. The stepwise CMD facilitates 3-D spatial variability modeling in probabilistic site characterization and routine geotechnical reliability analysis.

1. Introduction

Geomaterials exhibit three-dimensional (3-D) spatial variability, although such a variability is often simplified as one-dimensional (1-D) [10,32,36] or two-dimensional (2-D) [1,19,27] in practice. As geotechnical uncertainties and risk assessment draw increasing attention, the geotechnical community has recognized that the 3-D spatial variability of geomaterials significantly affects the failure mechanism and reliability of geotechnical structures (e.g., foundations [4,8,16] and slopes [13,20,33]) and cannot be completely represented by the simplified 1-D/2-D models. Hence it is necessary to incorporate the complete 3-D spatial variability into geotechnical reliability analysis, which is highly advocated in the latest international standard ISO2394:2015 Annex D (reliability of geotechnical structures) [23].

* Corresponding author.
E-mail addresses: dianqing@whu.edu.cn (D.-Q. Li), short_xiaote@whu.edu.cn (T. Xiao), cezhangl@ust.hk (L.-M. Zhang), zijuncao@whu.edu.cn (Z.-J. Cao).

https://doi.org/10.1016/j.apm.2018.11.011
0307-904X/

In geotechnical reliability analysis community, the spatial variability is often modeled as a random field [9]. Random field simulation is a crucial bridge linking the probabilistic site characterization [11,22,35] to the geotechnical reliability analysis and risk assessment [8,20,33]. Most random field simulation techniques are extendable from simple 1-D/2-D problems to complex 3-D cases, such as covariance matrix decomposition (CMD) [9], autoregressive moving-average [24], spectral representation [25], local average subdivision [6,7], circulant embedding [5], Karhunen–Loève expansion [37], and variants of linear estimation [21,33]. In spite of this, the 3-D random field simulation still faces challenges in practical implementation and computational efforts, particularly in simulating multivariate large-scale 3-D random fields. On the one hand, as the simplest and most widely-used approach in 1-D/2-D problems [17,18,38], CMD is theoretically applicable to 3-D problems but is rarely adopted. This is because the 3-D random field is usually associated with an extremely large spatial correlation matrix (e.g., the correlation matrix size of a $100 \times 100 \times 100$ random field is $10^6 \times 10^6$) and the decomposition of such a large matrix is both time-consuming and prone to considerable round-off errors [6]. On the other hand, other techniques need relatively complicated mathematical algorithms, not easy to implement by practitioners, and their computational efforts may also be prohibitive in large-scale 3-D random field simulations. For example, Liu et al. [21] reported that it takes about 20 minutes to generate one set of bivariate 3-D random fields with 10^6 nodes using the modified linear estimation method on a desktop computer, which is faster than the spectral representation method by about two to five orders of magnitude. Despite its improved efficiency, almost half a month is still required to prepare 1000 sets of realizations for reliability analysis such as random finite element method [9], which is prohibitive for practical applications.

To address the aforementioned difficulties in simulating multivariate large-scale 3-D random fields, this paper proposes a highly efficient approach, named stepwise CMD, for 3-D problems in which the correlation function is separable. It takes full advantage of the separability of correlation function and disassembles a large global correlation matrix into three small 1-D correlation matrices for each dimension. This allows the 3-D random fields to be generated in a stepwise manner with minimal computational efforts. The paper is organized as follows. The general CMD is briefly described first. Afterwards, the stepwise CMD is developed for 3-D random field simulation at both point and element levels, followed by an extension to multivariate random fields. Finally, the validity and efficiency of the proposed approach is illustrated through two large-scale 3-D examples and compared with some other random field generation techniques.

2. General covariance matrix decomposition

The CMD is the most widely-used random field generation approach due to its simplicity and accuracy. Without loss of generality, a standard normal random field $\boldsymbol{X}$ with n locations in space can be produced by [9]:

$$\boldsymbol{X} = \boldsymbol{L}\boldsymbol{U} \tag{1}$$

where $\boldsymbol{U} = n \times 1$ independent standard normal random vector; $\boldsymbol{L} = n \times n$ decomposition matrix satisfying $\boldsymbol{L}\boldsymbol{L}^{\mathrm{T}} = \boldsymbol{R}$, typically obtained using Cholesky decomposition or eigen-decomposition; and $\boldsymbol{R} = [\rho] = n \times n$ correlation matrix among all locations, whose element ρ is calculated by a prescribed correlation function. For standard normal distribution, the correlation matrix equals the covariance matrix because of the unit variance. Other non-normal random field can be obtained through isoprobabilistic transformation techniques, such as Nataf transformation [28,31].

Theoretically, Eq. (1) is applicable to 1-D, 2-D and 3-D problems with various correlation functions (e.g., single exponential [30], squared exponential [30], modified exponential [26], and Spartan [15,29]). For example, the simplest 1-D single exponential correlation function is defined as $\rho(\tau) = \exp(-2\tau/\delta)$, where $\tau =$ separation distance between two locations and $\delta =$ scale of fluctuation. Regarding the computational complexity of Eq. (1), if a standard Cholesky decomposition algorithm is employed, the matrix decomposition $\boldsymbol{L}\boldsymbol{L}^{\mathrm{T}} = \boldsymbol{R}$ and the random field realization $\boldsymbol{X} = \boldsymbol{L}\boldsymbol{U}$ require $\mathrm{O}(n^3)$ and $\mathrm{O}(n^2)$ floating point operations, respectively. The computational resources of the original CMD increase significantly as n increases, which limits its application to relatively small-scale univariate 3-D random fields. Simulating a 3-D random field with $n = 20 \times 20 \times 40$, for example, utilizes almost all the memory space of a 16 GB RAM desktop computer. This is far from being desired in practice. Since such a CMD is applicable to general correlation functions, it is referred to as the general CMD to distinguish itself from the stepwise CMD proposed in the next section.

3. Stepwise covariance matrix decomposition

3.1. Disassembly of correlation matrix for separable correlation function

As site-specific geotechnical data is usually sparse, for practical purpose, geotechnical reliability analysis community prefers to characterize the spatial variability of geomaterials with a simple correlation function [2,9,30]. Similarly, for multi-dimensional problems, a simple separable correlation function as the product of multiple directional 1-D correlation functions is frequently used in geotechnical literature (e.g., 2-D separable functions [1,18,27] and 3-D separable functions [4,11,33]), and it reads, with respect to a 3-D case, as

$$\rho(\tau_x, \tau_y, \tau_z) = \rho(\tau_x)\rho(\tau_y)\rho(\tau_z) \tag{2}$$

where τ_x, τ_y and $\tau_z =$ separation distances between two locations in the x-, y- and z-directions, respectively. For example, a 3-D separable version of the aforementioned single exponential correlation function is $\rho(\tau_x, \tau_y,$

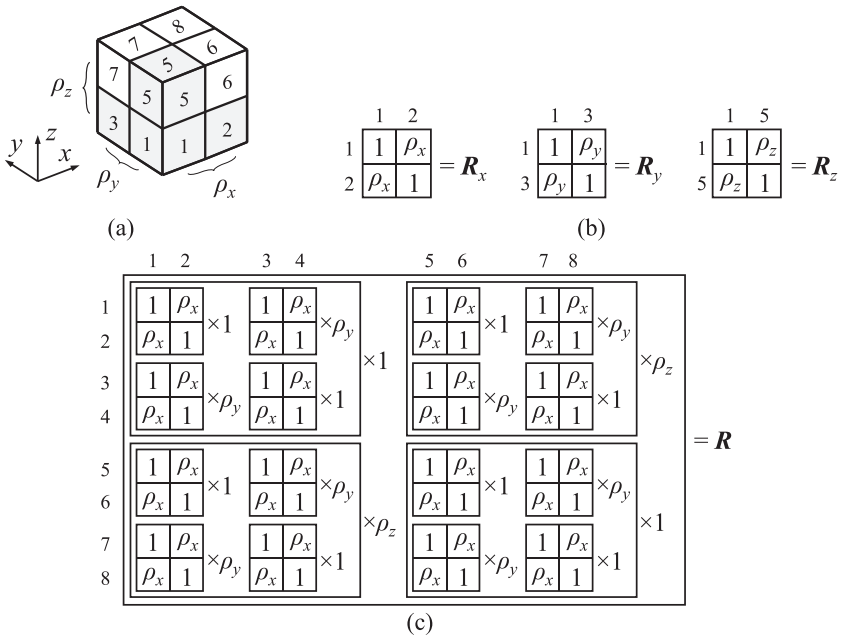

Fig. 1. Illustration of 3-D separable correlation matrix: (a) 3-D lattice and numbering sequence; (b) 1-D correlation matrices, $\boldsymbol{R}_x$, $\boldsymbol{R}_y$ and $\boldsymbol{R}_z$; (c) global correlation matrix, $\boldsymbol{R}$.

$\tau_z) = \exp(-2\tau_x/\delta_x - 2\tau_y/\delta_y - 2\tau_z/\delta_z)$, where δ_x, δ_y and δ_z = scales of fluctuation in the x-, y- and z-directions, respectively. Admittedly, the assumption on separability is quite simplified and may not always coincide with the reality. It nevertheless allows the correlation function to be identified in a single dimension (e.g., vertical direction) and matches the conventional procedure of probabilistic site characterization that individually identifies the vertical and horizontal correlation functions [2,11,35].

Consider a 3-D lattice with n_x, n_y and n_z locations in the x-, y- and z-directions, respectively (i.e., $n = n_x \times n_y \times n_z$). If these locations are organized in a particular sequence, namely along the x-, y- and z-directions successively as shown in Fig. 1(a), a global correlation matrix $\boldsymbol{R}$ associated with the separable correlation function can be disassembled into three 1-D correlation matrices as

$$\boldsymbol{R} = \boldsymbol{R}_z \otimes \boldsymbol{R}_y \otimes \boldsymbol{R}_x \tag{3}$$

where $\otimes$ = Kronecker product; and $\boldsymbol{R}_x$, $\boldsymbol{R}_y$ and $\boldsymbol{R}_z$ = 1-D correlation matrices in the x-, y- and z-directions, respectively. Compared with the $n \times n$ $\boldsymbol{R}$, these 1-D correlation matrices are much smaller in size (i.e., $n_x \times n_x$, $n_y \times n_y$, and $n_z \times n_z$, respectively). For illustration, Fig. 1 shows the disassembly of $\boldsymbol{R}$ using a $2 \times 2 \times 2$ lattice example. Applying the mixed-product property of the Kronecker product [14] to Eq. (3), it can be proved that

$$\boldsymbol{L} = \boldsymbol{L}_z \otimes \boldsymbol{L}_y \otimes \boldsymbol{L}_x \tag{4}$$

where $\boldsymbol{L}_x$, $\boldsymbol{L}_y$ and $\boldsymbol{L}_z$ = decomposition matrices satisfying $\boldsymbol{L}_x\boldsymbol{L}_x^T = \boldsymbol{R}_x$, $\boldsymbol{L}_y\boldsymbol{L}_y^T = \boldsymbol{R}_y$ and $\boldsymbol{L}_z\boldsymbol{L}_z^T = \boldsymbol{R}_z$, respectively. The direct decomposition of a large global correlation matrix is simplified and replaced by the decomposition of three small correlation matrices.

3.2. Stepwise random field realization

Substituting Eq. (4) into Eq. (1) gives

$$\boldsymbol{X} = (\boldsymbol{L}_z \otimes \boldsymbol{L}_y \otimes \boldsymbol{L}_x)\boldsymbol{U} \tag{5}$$

Note that $\boldsymbol{U}$ and $\boldsymbol{X}$ are $n_x n_y n_z \times 1$ vectors and $\boldsymbol{L} = \boldsymbol{L}_z \otimes \boldsymbol{L}_y \otimes \boldsymbol{L}_x$ is an $n_x n_y n_z \times n_x n_y n_z$ matrix. Although the correlation matrix decomposition is simplified through Kronecker product, the large matrix multiplication involved in Eq. (5) still restricts the 3-D random field generation. Instead, a stepwise strategy is applied in this study to supplant the large matrix multiplication.

Before moving to the stepwise strategy, let us first define a matrix-array multiplication operation "$\times_i$" over ith dimension of an array. In this study, array is referred to as a multi-dimensional data structure, and vector and matrix are the 1-D and 2-D special forms of array. Consider that $\underline{\boldsymbol{C}} = \boldsymbol{A} \times_i \underline{\boldsymbol{B}}$ for example, in which $\boldsymbol{A} = [a]$ is a square matrix, and $\underline{\boldsymbol{B}} = [b]$ and $\underline{\boldsymbol{C}} = [c]$ are multi-dimensional arrays with the same array size. In the matrix-array multiplication operation, each entry of $\underline{\boldsymbol{C}}$ is given

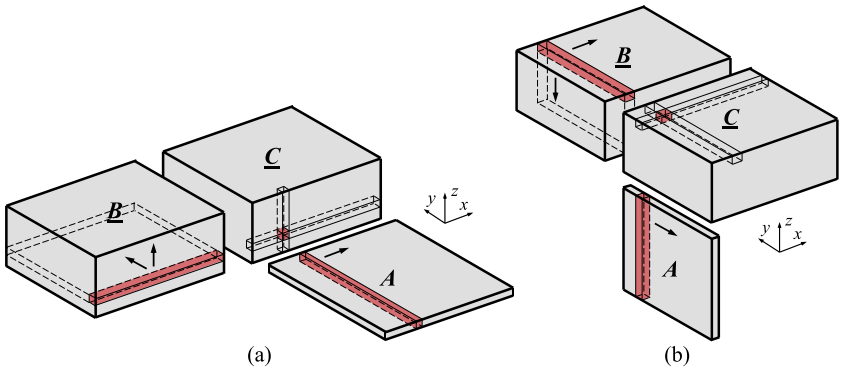

Fig. 2. Illustration of matrix-array multiplication for 3-D array: (a) $\underline{\boldsymbol{C}}=A\times_1\underline{\boldsymbol{B}}$; (b) $\underline{\boldsymbol{C}}=A\times_2\underline{\boldsymbol{B}}$

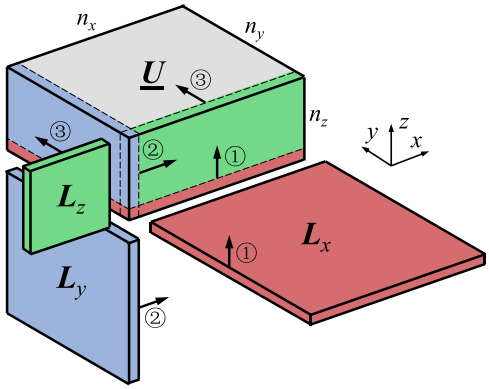

Fig. 3. Schematic diagram of 3-D random field simulation using stepwise CMD.

by multiplying all entries along the second dimension of $\boldsymbol{A}$ by the entries along the ith dimension of $\underline{\boldsymbol{B}}$ and summing up the results. Intuitively, it appears like that the first dimension of the matrix takes the place of the ith dimension of the array. Particularly with respect to 3-D arrays $\underline{\boldsymbol{B}}$, $\underline{\boldsymbol{C}}=\boldsymbol{A}\times_i\underline{\boldsymbol{B}}$ is calculated as $c_{jpq}=\sum_k a_{jk}b_{kpq}$ if $i=1$, $c_{pjq}=\sum_k a_{jk}b_{pkq}$ if $i=2$, and $c_{pqj}=\sum_k a_{jk}b_{pqk}$ if $i=3$; with respect to 2-D array $\boldsymbol{B}$ (or matrix $\boldsymbol{B}$), the calculation is equivalent to $\boldsymbol{A}\times_1\boldsymbol{B}=\boldsymbol{AB}$ and $\boldsymbol{A}\times_2\boldsymbol{B}=\boldsymbol{BA}^{\mathrm{T}}$. For better understanding, Fig. 2 illustrates diagrammatically the matrix-array multiplication for 3-D array.

With the help of the matrix-array multiplication operation, Eq. (5) can be rewritten in a stepwise but equivalent form as

$$\underline{\boldsymbol{X}}=\boldsymbol{L}_z\times_3[\boldsymbol{L}_y\times_2(\boldsymbol{L}_x\times_1\underline{\boldsymbol{U}})] \tag{6}$$

where $\underline{\boldsymbol{U}}$ and $\underline{\boldsymbol{X}}=n_x\times n_y\times n_z$ arrays reshaped from $n_xn_yn_z\times 1$ vectors $\boldsymbol{U}$ and $\boldsymbol{X}$, respectively. Concretely, $\underline{\boldsymbol{U}}=[u_{ijk}]$, $\boldsymbol{U}=[u_p]$, and $u_{ijk}=u_p$ for $p=i+(j-1)n_x+(k-1)n_xn_y$ ($i=1,2,\ldots,n_x$; $j=1,2,\ldots,n_y$; $k=1,2,\ldots,n_z$). Eq. (6) generates the 3-D random field step-by-step and each step realizes the spatial correlation in one single dimension, thus referred to as stepwise CMD. It can be applied to large-scale 3-D random field simulation due to the avoidance of large matrix multiplication in Eq. (5). A rigorous proof of the equivalence between Eqs. (5) and (6) is provided in Appendix A. It guarantees that the stepwise CMD is capable of generating strictly accurate random field as the general CMD is.

In substance, the matrix-array multiplication operation cuts an array into pieces of matrices and performs matrix multiplication piece by piece, as shown in Fig. 2. From this perspective, Eq. (6) has a more explicit meaning as shown in Fig. 3, namely $\underline{\boldsymbol{U}}$ is multiplied by $\boldsymbol{L}_x$, $\boldsymbol{L}_y$ and $\boldsymbol{L}_z$ sequentially along each single dimension. The extremely large matrices $\boldsymbol{R}$ and $\boldsymbol{L}$ taking the most computational memory space in the general CMD are totally bypassed. Although the matrix-array multiplication operation appears to be complicated, it is trivial to be transformed into multiple matrix multiplication operations. By this means, the implementation of the stepwise CMD is as easy as that of the general CMD and can be realized using only a few lines of Matlab code, as demonstrated in Fig. 4. The stepwise CMD spends $\mathrm{O}(n_x^3+n_y^3+n_z^3)$ floating point operations on decomposing three 1-D correlation matrices and $\mathrm{O}[n_xn_yn_z(n_x+n_y+n_z)]$ floating point operations on generating random fields. It not only inherits the simplicity of the general CMD, but also significantly minimizes the computational complexity. As summarized in Table 1, especially for matrix decomposition, the number of floating point operations and the required memory space fall by 11 and 7 orders of magnitude, respectively, for a $100\times100\times100$ random field using the stepwise CMD. This would facilitate the 3-D spatial variability modeling in large-scale geotechnical reliability analysis.

```
U = randn(nx, ny, nz);          % nx-ny-nz array
X = Lx*reshape(U, nx, ny*nz); % nx-ny*nz matrix
X = reshape(X, nx, ny, nz);    % nx-ny-nz array
X = permute(X, [2, 3, 1]);     % ny-nz-nx array
X = Ly*reshape(X, ny, nz*nx); % ny-nz*nx matrix
X = reshape(X, ny, nz, nx);    % ny-nz-nx array
X = permute(X, [2, 3, 1]);     % nz-nx-ny array
X = Lz*reshape(X, nz, nx*ny); % nz-nx*ny matrix
X = reshape(X, nz, nx, ny);    % nz-nx-ny array
X = permute(X, [2, 3, 1]);     % nx-ny-nz array
```

Fig. 4. Implementation of stepwise CMD in Matlab.

Table 1
Summary of CMD for 3-D random field simulation.

Method	Applicability	Computational complexity		
			Matrix decomposition	Random field realization
General CMD	General correlation function	Formula	$\boldsymbol{L}\boldsymbol{L}^{\mathrm{T}}=\boldsymbol{R}$	$\boldsymbol{X}=\boldsymbol{L}\boldsymbol{U}$
		FLOPs[a]	$O[(n_x n_y n_z)^3]$ ($\approx 10^{18}$)[c]	$O[(n_x n_y n_z)^2]$ ($\approx 10^{12}$)[c]
		Memory space[b]	$O[(n_x n_y n_z)^2]$ (≈ 7.3 TB)[c]	$O(n_x n_y n_z)$ (≈ 7.6 MB)[c]
Stepwise CMD	Separable correlation function	Formula	$\boldsymbol{L}_x\boldsymbol{L}_x^{\mathrm{T}}=\boldsymbol{R}_x$, $\boldsymbol{L}_y\boldsymbol{L}_y^{\mathrm{T}}=\boldsymbol{R}_y$, $\boldsymbol{L}_z\boldsymbol{L}_z^{\mathrm{T}}=\boldsymbol{R}_z$	$\underline{\boldsymbol{X}}=\boldsymbol{L}_z\times_3[\boldsymbol{L}_y\times_2(\boldsymbol{L}_x\times_1\underline{\boldsymbol{U}})]$
		FLOPs[a]	$O(n_x^3+n_y^3+n_z^3)$ ($\approx 3\times 10^6$)[c]	$O[n_x n_y n_z(n_x+n_y+n_z)]$ ($\approx 3\times 10^8$)[c]
		Memory space[b]	$O(n_x^2+n_y^2+n_z^2)$ (≈ 0.2 MB)[c]	$O(n_x n_y n_z)$ (≈ 7.6 MB)[c]

[a] FLOPs = floating point operations.
[b] Required memory space for $\boldsymbol{R}$ in the stage of matrix decomposition and that for $\boldsymbol{U}$ in the stage of random field realization.
[c] Evaluated assuming $n_x = n_y = n_z = 100$.

3.3. Generation of spatially averaged random fields

Notably, the aforementioned 3-D random field simulation is achieved at the point level. For 3-D random fields at the element level, such as those involved in random finite element method [9], the impact of spatial average on statistics and correlations should be considered.

According to the random field theory [30], the spatially averaged random field has an unchanged mean and a reduced variance in comparison with the point-level random field. The variance reduction factor γ is evaluated by a variance reduction function and depends on element sizes, namely $\gamma(D_x, D_y, D_z)$, where D_x, D_y and D_z = element sizes in the x-, y- and z-directions, respectively. Besides, the element-level random field also holds the spatial correlation ρ_E among different elements, relying on centroid separation distances and element sizes, namely $\rho_E(T_x, T_y, T_z, D_x, D_y, D_z)$, where T_x, T_y and T_z = centroid separation distances between two elements in the x-, y- and z-directions, respectively. Both the variance reduction function and the element correlation function are related to the prescribed correlation function, and they are also separable given a separable correlation function:

$$\begin{cases}\gamma(D_x, D_y, D_z) = \gamma(D_x)\gamma(D_y)\gamma(D_z)\\ \rho_E(T_x, T_y, T_z, D_x, D_y, D_z) = \rho_E(T_x, D_x)\rho_E(T_y, D_y)\rho_E(T_z, D_z)\end{cases} \tag{7}$$

where the 1-D element correlation can be evaluated as [30]

$$\rho_E(T, D) = \frac{\Delta(T-D)+\Delta(T+D)-2\Delta(T)}{2\Delta(D)} \tag{8}$$

where $\Delta(T) = T^2\gamma(T)$.

Again, owing to the separability of element correlation function, the global correlation matrix at the element level can be disassembled into three 1-D correlation matrices as well so that Eq. (6) can be applied to generate the 3-D spatially averaged random fields efficiently. In the context of CMD, the random field simulations at the point and element levels only differ in the input statistics and correlations. The element-level simulation is theoretically more rigorous due to a proper consideration of spatial average. The difference between the point-level and element-level simulations is negligible if the element size is significantly smaller than the scale of fluctuation.

4. Extension to multivariate random fields

Although the univariate random field fulfills most practical needs in geotechnical spatial variability modeling, it is still not uncommon to deal with multivariate cross-correlated random fields, such as the cohesion and friction of the same soil.

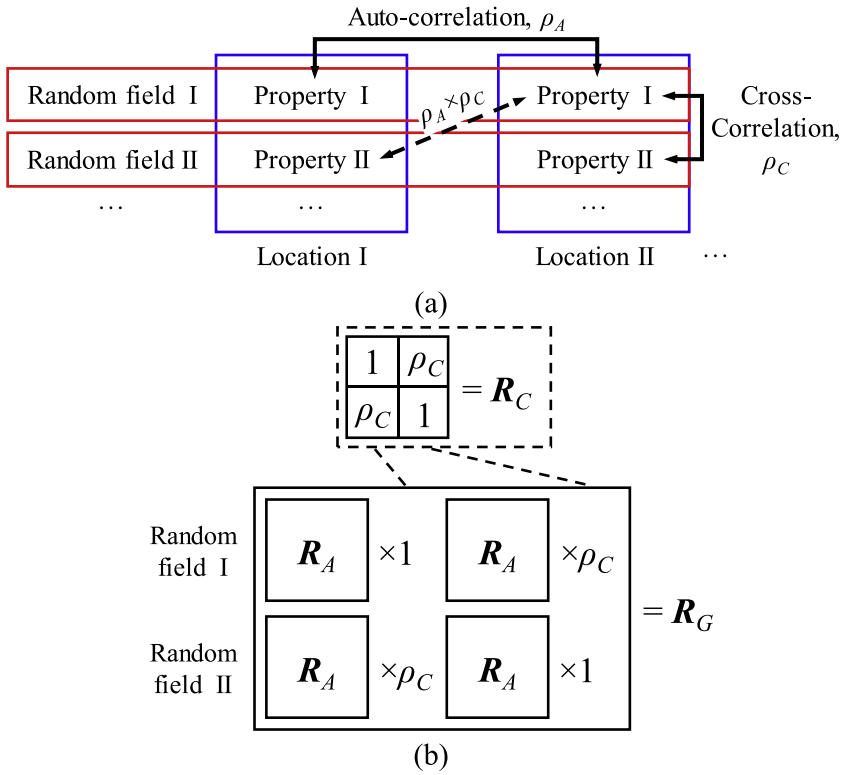

Fig. 5. Correlations in multivariate random fields: (a) simplified model; (b) correlation matrix.

Two different types of correlation exist in the multivariate case, as illustrated in Fig. 5(a). One is auto-correlation, which represents the spatial correlation among the values of a soil property at different locations and is characterized by an auto-correlation function and scales of fluctuation, as discussed in previous sections. Subject to the same natural process in history, correlation functions and scales of fluctuation for different properties of the same soil are often assumed to be consistent. Another is cross-correlation, denoting the correlation between different soil properties at the same location. It is usually described by cross-correlation coefficients, instead of a cross-correlation function, due to the limited data in geotechnical practice [3,21,38]. For simplicity, the correlation among multiple random fields at different locations is conventionally decoupled as the product of cross-correlation and auto-correlation [31,34,38], as shown in Fig. 5.

By this means, the global correlation matrix $\boldsymbol{R}_G$ and its decomposition matrix $\boldsymbol{L}_G$ can be rewritten in form of the Kronecker product, analogous to Eqs. (3) and (4), as

$$\begin{cases} \boldsymbol{R}_G = \boldsymbol{R}_C \otimes \boldsymbol{R}_A \\ \boldsymbol{L}_G = \boldsymbol{L}_C \otimes \boldsymbol{L}_A \end{cases} \tag{9}$$

where $\boldsymbol{R}_C$ and $\boldsymbol{R}_A$ = cross- and auto-correlation matrices, respectively; and $\boldsymbol{L}_C$ and $\boldsymbol{L}_A$ = decomposition matrices satisfying $\boldsymbol{L}_C\boldsymbol{L}_C^T = \boldsymbol{R}_C$ and $\boldsymbol{L}_A\boldsymbol{L}_A^T = \boldsymbol{R}_A$, respectively. Applying the equivalent transformation for the Kronecker product [14] to Eq. (1), the general multivariate cross-correlated random fields can be obtained by

$$\underline{\boldsymbol{X}} = \boldsymbol{L}_A\underline{\boldsymbol{U}}\boldsymbol{L}_C^{\mathrm{T}} \tag{10}$$

where $\underline{\boldsymbol{U}}$ and $\underline{\boldsymbol{X}} = n \times n_p$ matrices; and n_p = number of soil properties. If a separable 3-D auto-correlation function is further considered, $\boldsymbol{R}_A$ can be substituted with $\boldsymbol{R}$ in Eq. (3) and $\boldsymbol{R}_G$ becomes a four-dimensional upgrade of Eq. (3), where the soil property is the fourth dimension. Therefore, the simulation of multivariate cross-correlated 3-D random fields can be achieved using the stepwise CMD by

$$\underline{\boldsymbol{X}} = \boldsymbol{L}_C \times_4 \{\boldsymbol{L}_z \times_3 [\boldsymbol{L}_y \times_2 (\boldsymbol{L}_x \times_1 \underline{\boldsymbol{U}})]\} \tag{11}$$

where $\underline{\boldsymbol{U}}$ and $\underline{\boldsymbol{X}} = n_x \times n_y \times n_z \times n_p$ arrays. Similar to the univariate case, Eq. (11) as a multivariate extension of Eq. (6) is equivalent to Eq. (10). Since n_p is much smaller than n_x, n_y or n_z, the computational effort of Eq. (11) is almost n_p times the effort of the univariate 3-D random field simulation using Eq. (6). This is, again, much less than the general CMD that requires at least n_p^2 times. The stepwise CMD simplifies the simulation of multivariate random fields by producing the auto- and cross-correlations in a consistent stepwise manner, which is another advantage of the stepwise CMD in comparison with other random field generation approaches.

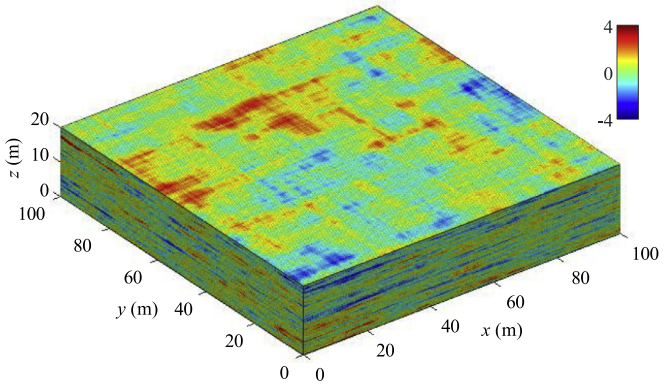

Fig. 6. Example of 3-D random field realization ($201 \times 201 \times 401$).

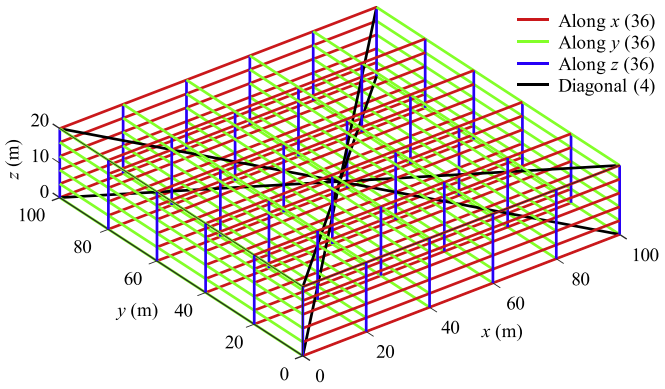

Fig. 7. Selected paths for validation.

5. Illustrative examples

This section applies the stepwise CMD to simulate large-scale and high-resolution 3-D random fields, such as a site investigated by a large amount of piezocone penetration tests (CPTu). A 3-D separable single exponential correlation function is used to describe the spatial variability of soil properties with prescribed scales of fluctuation $[\delta_x, \delta_y, \delta_z] = [30, 20, 1]$ m. The 3-D random field domain measures 100 m × 100 m × 20 m in space with grid intervals of 0.5 m, 0.5 m and 0.05 m in the x-, y- and z-directions, respectively, leading to a total of $n = 201 \times 201 \times 401 \approx 1.6 \times 10^7$ nodes. The global correlation matrix $\boldsymbol{R}$ among all locations is 1.6×10^7-by-1.6×10^7 in size, which is too large to decompose using the general CMD.

5.1. Univariate 3-D random field

For better validation, a univariate 3-D random field with a standard normal distribution is considered first. In the context of the stepwise CMD, the 1-D correlation matrices in the x-, y- and z-directions, namely $\boldsymbol{R}_x$ (201×201 in size), $\boldsymbol{R}_y$ (201×201 in size) and $\boldsymbol{R}_z$ (401×401 in size), can be decomposed easily with negligible efforts. They then sequentially act on a 3-D independent random array ($201 \times 201 \times 401$ in size) using Eq. (6) to obtain a 3-D random field. An example is given in Fig. 6, which only demands 0.65 s, including both matrix decomposition and one random field realization, on a desktop computer with 16 GB RAM and one Intel Core i7 CPU clocked at 3.4 GHz. In spite of the large-scale and high-resolution nature of the 3-D random field, the stepwise CMD is still computationally efficient and satisfies practical requirements.

To validate the accuracy of the stepwise CMD, 100 random realizations are repeatedly produced. Afterwards, the spatial correlations along some specific paths are estimated using statistical analysis and compared against the corresponding true ones calculated using the prescribed correlation function. For illustration, 36, 36, 36 and 4 paths along the x-, y-, z- and diagonal directions, respectively, are selected as shown in Fig. 7. The estimated correlation functions of the simulated data and their averages are plotted in Fig. 8 by light and dark solid lines, respectively. The true correlation functions are also given in Fig. 8 by dashed lines for reference. The averages agree well with the true functions in all directions. Similarly, the estimated correlation functions along the other arbitrary paths not contained in Fig. 7 converge to their targets as well, indicating the validity of the stepwise CMD.

Furthermore, take the considered random field as a benchmark, and then downscale the benchmark by 2, 5, 10, 20 and 50 times in all three directions to construct relatively low-resolution random fields (i.e., $n \approx 2.1 \times 10^6$, 1.4×10^5, 1.8×10^4, 2541,

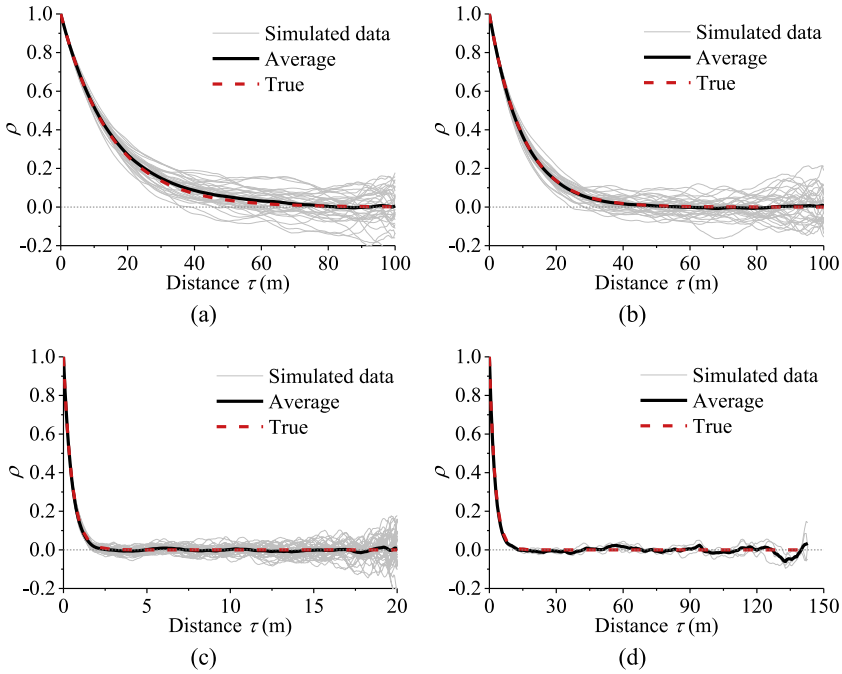

Fig. 8. Validation of spatial correlations along different directions: (a) *x*-direction; (b) *y*-direction; (c) *z*-direction; (d) diagonal direction.

and 225, respectively) and upscale it by 2 and 2.5 times to form higher-resolution ones (i.e., $n \approx 2.5 \times 10^8$ and 2.0×10^9, respectively). As a result, there are eight scenarios in total including the benchmark. To make a better comparison, the circulant embedding method (CEM) [5] and Karhunen–Loève expansion (KLE) [12] are also investigated in addition to the two CMDs. The CEM and KLE approaches are well-known for their efficiency and accuracy but call for more complicated algorithms. Fig. 9 compares the required memory space with regard to correlation matrix $\boldsymbol{R}$ (solid lines in Fig. 9(a)) and random variable $\boldsymbol{U}$ (dashed lines in Fig. 9(a)), as well as the computational times for matrix decomposition (solid lines in Fig. 9(b)) and one random field realization (dashed lines in Fig. 9(b)) for the eight scenarios. Notably, computational memory space for $\boldsymbol{R}$ is $O[(n_x n_y n_z)^2]$ in the general CMD and $O(n_x^2 + n_y^2 + n_z^2)$ in the stepwise CMD, and that for $\boldsymbol{U}$ is $O(n_x n_y n_z)$ in both of them. As for the CEM, in order to apply the fast Fourier transform to matrix decomposition [5], the 3-D domain is deliberately doubled in all directions to embed $\boldsymbol{R}$ into a circulant matrix, and $\boldsymbol{U}$ is comprised of both real and imaginary parts. Hence the required memory space is $O(8n_x n_y n_z)$ for $\boldsymbol{R}$ and is further doubled for $\boldsymbol{U}$. Since the CEM gains 16 realizations within one simulation, the average time is used in Fig. 9(b) for fair comparison. Regarding the KLE, eigenvalues and eigenvectors of each 1-D correlation matrix are calculated analytically and then used to form eigenvalues and eigenvectors of the 3-D correlation matrix through product [12]. The formation of 3-D eigenvalues and eigenvectors is valid also because of the separability of correlation function. In the case of single exponential correlation function, the KLE demands enormous expansion terms to reach a certain accuracy. For the sake of the success of KLE, the 3-D domain size is deliberately reduced by 20 times in all directions, and 100 expansion terms are truncated to ensure the eigenvalue ratio [31] over 95%. All the 100 eigenvalues and eigenvectors are simultaneously reserved to avoid repeated evaluation of them in every random field realization. In Fig. 9(a), consumed memory space for $\boldsymbol{R}$ in the KLE is represented by that for eigenvalues and eigenvectors, i.e., $O(100 n_x n_y n_z)$, and consumed memory space for $\boldsymbol{U}$ remains unchanged for all scenarios, i.e., O(100). It should be highlighted that the computational resources of KLE rely on its implementation manner and various problem-dependent factors (e.g., scales of fluctuation, domain sizes, differentiability of correlation function), not merely the number of nodes, thus the results of KLE are for reference only.

The maximum allocable memory space for $\boldsymbol{R}$ or $\boldsymbol{U}$ is approximately 2 GB on a 16 GB RAM desktop computer. Surpassing this limit may have an “out of memory” issue and cannot produce the random field successfully. As shown in Fig. 9, the stepwise CMD performs best, followed by the CEM and KLE, not only in terms of the computational resources (i.e., memory space and time), but also in terms of the growth rate with the increasing problem scale. The general CMD fails when the resolution of random field exceeds $21 \times 21 \times 41$, which is insufficient to describe large-scale 3-D random fields, and the KLE and CEM fail after $101 \times 101 \times 201$ and $201 \times 201 \times 401$, respectively. In contrast, the stepwise CMD needs much less memory space and still works well when the resolution is as high as $501 \times 501 \times 1001$. The required memory space of $\boldsymbol{R}$ in the stepwise CMD is about 4.2×10^{10}, 17,000 and 1300 times less than that in the general CMD, KLE and CEM, respectively. By applying the stepwise manner to CMD, the maximum resolution of random field is significantly improved by about 15,000 times and suffices in most engineering applications. With regards to the computational efficiency, the time

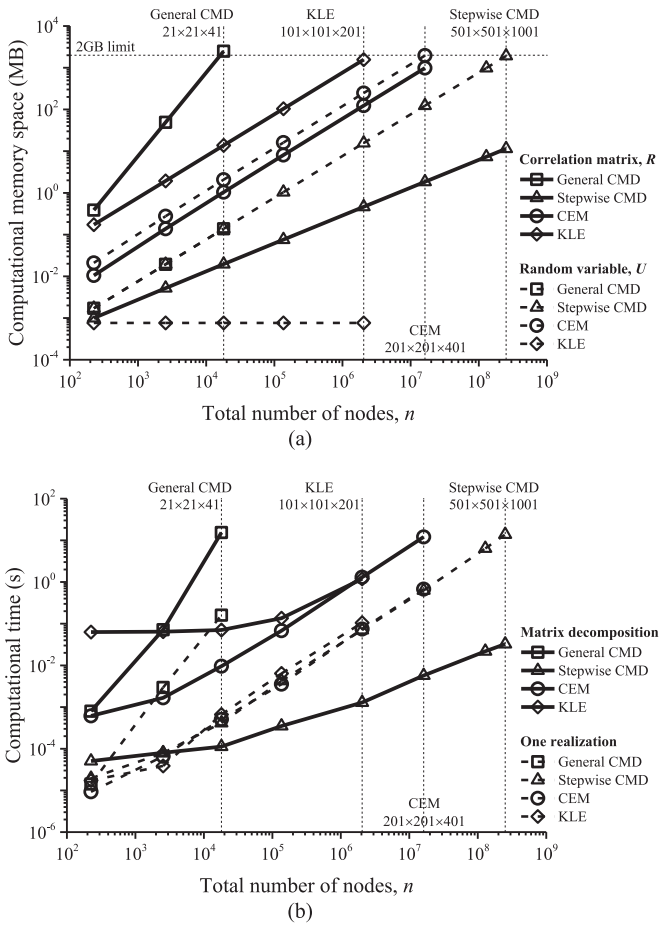

Fig. 9. Comparison of computational efforts among different methods: (a) required memory space for correlation matrix (***R***) and random variable (***U***); (b) computational time for matrix decomposition and one random field realization.

for random field realization is concerned in geotechnical reliability analysis because thousands of realizations are usually needed. In this aspect, the stepwise CMD, CEM and KLE perform equally well and much better than the general CMD. If the 3-D random field simulation is a part of the probabilistic site characterization (e.g., [35]), the time for matrix decomposition is also of interest. The stepwise CMD only takes 1/140,000, 1/2100 and 1/900 of the decomposition times required by the general CMD, CEM and KLE, respectively, at their limit resolutions. As a result, the stepwise CMD significantly reduces the computational efforts in terms of both time and required memory space, particularly in large-scale and high-resolution 3-D random field simulations.

5.2. Trivariate random fields of CPTu parameters

To further showcase its capacities, the stepwise CMD is used to simulate trivariate random fields of CPTu parameters, including pore pressure ratio $B_q=(u_2-u_0)/(q_t-\sigma_v)$, normalized cone resistance $Q_t=(q_t-\sigma_v)/\sigma'_v$, and normalized effective cone resistance $Q_e=(q_t-u_2)/\sigma'_v$, where q_t = corrected cone resistance; u_2 = pore pressure behind the cone; σ_v = vertical total stress; σ'_v = vertical effective stress; and u_0 = static pore pressure. These parameters are correlated to a certain degree and are essential to the CPTu-based geotechnical design. Ching and Phoon [3] performed a multivariate statistical analysis of these parameters based on a global database of clays, as shown in Table 2, where Q_t and Q_e are in logarithm forms (i.e., $\ln Q_t$ and $\ln Q_e$). All the three CPTu parameters follow the unbounded Johnson distributions, among which $\ln Q_t$ and $\ln Q_e$ are positively correlated and both of them are negatively correlated with B_q. The isoprobabilistic transformation between an unbounded Johnson random variable Y and a standard normal random variable X is written as $Y=\sinh[(X-b_X)/a_X]\times a_Y+b_Y$ [3], where a_X, b_X, a_Y and b_Y are four distribution parameters.

Consider that both the 3-D spatial variability of the CPTu parameters (i.e., 3-D separable single exponential correlation function with $[\delta_x, \delta_y, \delta_z]=[30, 20, 1]$ m) and the 3-D random field domain (i.e., 100 m × 100 m × 20 m with grid intervals of 0.5 m, 0.5 m and 0.05 m, respectively) coincide with those in the previous example. By means of the stepwise CMD, the independent standard normal $\boldsymbol{U}$ ($201\times201\times401\times3$ in size) first yields correlated standard normal $\boldsymbol{X}$ (including both

Table 2
Statistics of three CPTu parameters (adapted from [3]).

CPTu parameter	Distribution type	Distribution parameters				Cross-correlation matrix in X-space		
		a_X	b_X	a_Y	b_Y			
B_q	Unbounded Johnson[a]	2.676	0.161	0.513	0.615	1	−0.45	−0.63
$\ln Q_t$		1.340	−0.572	0.659	1.476	−0.45	1	0.74
$\ln Q_e$		2.134	−1.102	1.154	0.657	−0.63	0.74	1

[a] Unbounded Johnson random variable $Y = \sinh[(X - b_X)/a_X] \times a_Y + b_Y$, where X is a standard normal random variable.

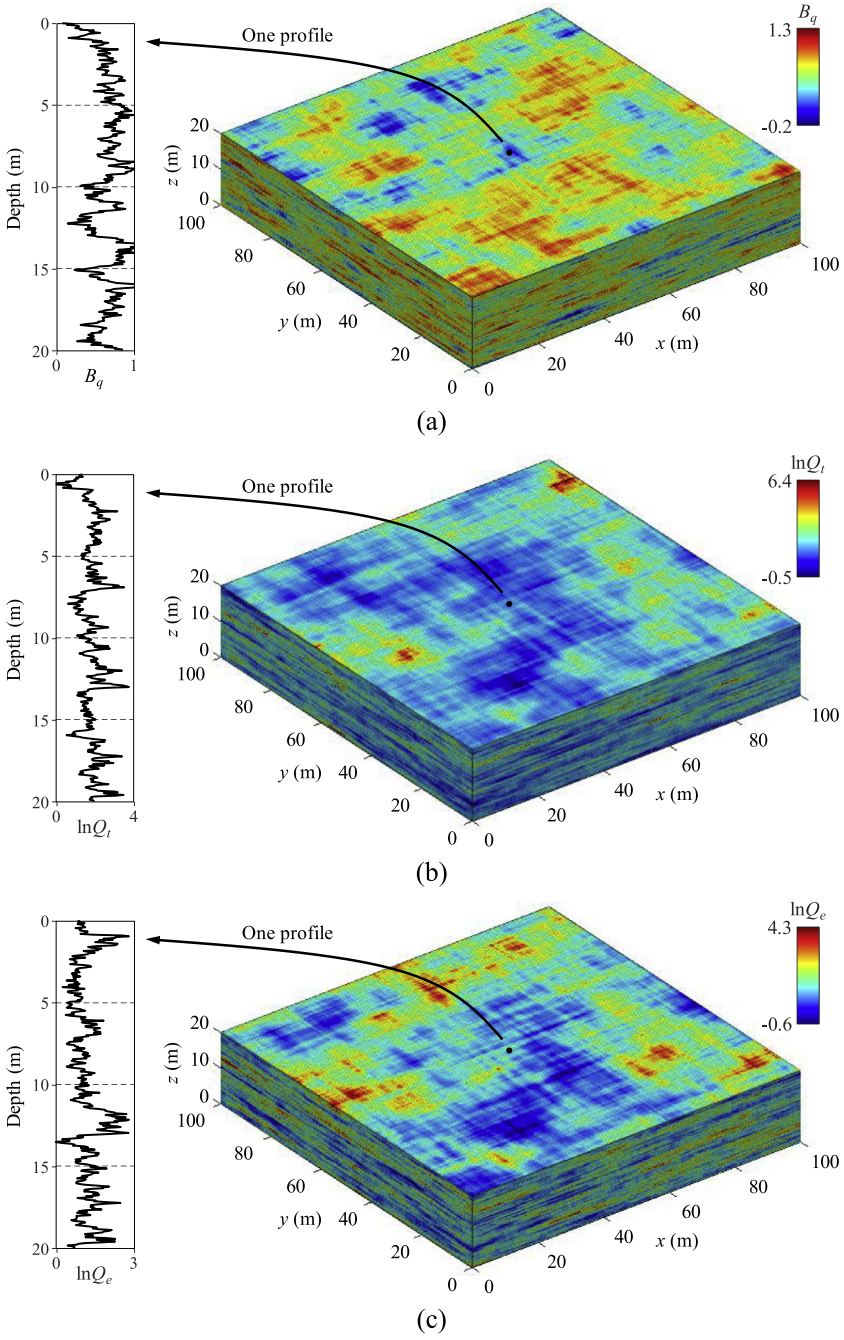

Fig. 10. One set of trivariate 3-D random fields of CPTu parameters: (a) B_q; (b) $\ln Q_t$; (c) $\ln Q_e$.

auto- and cross-correlations) using Eq. (11), and is then transformed to $\boldsymbol{Y}$ that follows the unbounded Johnson distribution. As shown in Fig. 10, a set of trivariate random fields with 1.6×10^7 nodes is realized in about 2.7 s using the stepwise CMD. Its unit efficiency, defined as $n \times n_p$ over the computational time, is nearly 10,000 times higher than that (i.e., 20 minutes for bivariate random fields with 10^6 nodes on a desktop computer with similar configurations) using the modified linear estimation method [21]. Also observed in Fig. 10, $\ln Q_t$ and $\ln Q_e$ have negative correlations with B_q but are positively correlated. To quantitatively estimate the cross-correlations, 10,000 locations are randomly selected from the 3-D random field domain. Based on multivariate statistical analysis, the cross-correlation coefficients between B_q and $\ln Q_t$, B_q and $\ln Q_e$, and $\ln Q_t$ and $\ln Q_e$ in the X-space are estimated as -0.45, -0.62 and 0.73, respectively, which agree well with the input cross-correlation coefficients (i.e., -0.45, -0.63 and 0.74) in Table 2. This validates the feasibility of the stepwise CMD in simulating multivariate cross-correlated random fields. By virtue of the stepwise CMD, it is possible to incorporate the complicated 3-D spatial variability of soil properties into routine geotechnical reliability analysis, rather than adopting the conventional 1-D/2-D simplification.

6. Summary and conclusions

This paper proposes a stepwise covariance matrix decomposition method (CMD) for multivariate large-scale three-dimensional (3-D) random field simulation with separable correlation functions. The primary idea is to disassemble the large global correlation matrix into small one-dimensional correlation matrices by taking the advantage of the separability of correlation function and to generate 3-D random fields sequentially along each single dimension. Two large-scale and high-resolution 3-D examples are investigated to validate the stepwise CMD and to benchmark the proposed method against other random field generation techniques. Several conclusions can be drawn from this study:

(1) The stepwise CMD is a theoretically rigorous random field simulation technique because of its mathematical equivalence to the general CMD. It can be easily implemented for multi-dimensional random field simulation at both point and element levels, and extended to multivariate random fields by modeling the auto- and cross-correlations in a consistent manner.
(2) The stepwise CMD not only inherits the simplicity of the general CMD, but also significantly reduces the computational efforts in terms of both time and required memory space. These advantages make it feasible for simulating large-scale and high-resolution 3-D random fields and eventually facilitate the 3-D spatial variability modeling in probabilistic site characterization and routine geotechnical reliability analysis. In the demonstrated large-scale examples, the stepwise CMD is conducted in few seconds, with the requirement on memory space reduced by more than ten orders of magnitude. The maximum resolution of 3-D random field is thus significantly improved from $21 \times 21 \times 41$ using the general CMD to $501 \times 501 \times 1001$ using the stepwise CMD, which suffices in most engineering applications.
(3) The stepwise CMD also performs better than the circulant embedding method, Karhunen–Loève expansion, and modified linear estimation method for large-scale problems. The univariate example shows that the stepwise CMD consumes less computational efforts than the circulant embedding method and Karhunen-Loève expansion, and the resource requirements increase more slowly with the problem scale. The trivariate example indicates that the unit efficiency of the stepwise CMD is nearly 10,000 times higher than that using the modified linear estimation method.

Acknowledgments

This work was supported by the National Key R&D Program of China (2017YFC1501301), the Research Grants Council of the Hong Kong Special Administrative Region (Project Nos. 16202716 and C6012-15G), and the National Natural Science Foundation of China (Project Nos. 51779189 and 51679174). The second author wishes to thank the Department of Civil and Environmental Engineering, The Hong Kong University of Science and Technology, for hosting his visit as an exchange Ph.D. student.

Appendix A. Proof of equivalence between general CMD and stepwise CMD

Let $\boldsymbol{L}_x = [a_{ij}]_{n_x \times n_x}$ denote an $n_x \times n_x$ matrix $\boldsymbol{L}_x$ with entries a_{ij}. Similarly, $\boldsymbol{L}_y = [b_{ij}]_{n_y \times n_y}$, $\boldsymbol{L}_z = [c_{ij}]_{n_z \times n_z}$, $\boldsymbol{L} = [l_{ij}]_{n_x n_y n_z \times n_x n_y n_z}$, $\boldsymbol{U} = [u_i]_{n_x n_y n_z \times 1}$ and $\boldsymbol{X} = [x_i]_{n_x n_y n_z \times 1}$. Besides, $\underline{\boldsymbol{U}} = [u_{ijk}]_{n_x \times n_y \times n_z}$ and $\underline{\boldsymbol{X}} = [x_{ijk}]_{n_x \times n_y \times n_z}$ are 3-D arrays reshaped from $\boldsymbol{U}$ and $\boldsymbol{X}$, respectively, with sequence along the x-, y- and z-directions successively. The matrix reshaping leads to $u_{ijk} = u_p$ and $x_{ijk} = x_p$ for $p = i + (j-1)n_x + (k-1)n_x n_y$.

Recall Eq. (4) that $\boldsymbol{L} = \boldsymbol{L}_z \otimes \boldsymbol{L}_y \otimes \boldsymbol{L}_x$. According to the rule of matrix multiplication, the Kronecker product for $\boldsymbol{L}$ is calculated as

$$l_{pq} = c_{kt} b_{js} a_{ir} \tag{12}$$

where $p = i + (j-1)n_x + (k-1)n_x n_y$ and $q = r + (s-1)n_x + (t-1)n_x n_y$. Therefore, the 3-D random field simulation using the general CMD (i.e., Eq. (5) or (1)) can be written as

$$x_p = \sum_{q=1}^{n_x n_y n_z} l_{pq} u_q = \sum_{t=1}^{n_z} \sum_{s=1}^{n_y} \sum_{r=1}^{n_x} \left(c_{kt} b_{js} a_{ir}\right) u_q \tag{13}$$

Similarly, according to the defined matrix-array multiplication operation, the 3-D random field simulation using the stepwise CMD (i.e., Eq. (6)) can be expressed as

$$x_{ijk} = \sum_{t=1}^{n_z} c_{kt} \left[\sum_{s=1}^{n_y} b_{js} \left(\sum_{r=1}^{n_x} a_{ir} u_{rst} \right) \right] = \sum_{t=1}^{n_z} \sum_{s=1}^{n_y} \sum_{r=1}^{n_x} c_{kt} \left[b_{js} (a_{ir} u_{rst}) \right] \tag{14}$$

Because of the fact that $x_{ijk} = x_p$ and $u_{rst} = u_q$ during the matrix reshaping, Eqs. (13) and (14) are always equivalent; so are Eqs. (5) and (6). Such an equivalent transformation between Eqs. (5) and (6) is a 3-D upgrade of the 2-D equivalent transformation for the Kronecker product (see Lemma 4.3.1 [14]). It guarantees the identical 3-D random fields generated by the general CMD and the stepwise CMD.

References

[1] A. Ali, A.V. Lyamin, J. Huang, S.W. Sloan, M.J. Cassidy, Undrained stability of a single circular tunnel in spatially variable soil subjected to surcharge loading, Comput. Geotech. 84 (2017) 16–27, doi:10.1016/j.compgeo.2016.11.013.

[2] Z. Cao, Y. Wang, Bayesian model comparison and selection of spatial correlation functions for soil parameters, Struct. Saf. 49 (2014) 10–17, doi:10.1016/j.strusafe.2013.06.003.

[3] J. Ching, K.K. Phoon, Correlations among some clay parameters—the multivariate distribution, Can. Geotech. J. 51 (6) (2014) 686–704, doi:10.1139/cgj-2013-0353.

[4] J. Ching, K.K. Phoon, Y.K. Pan, On characterizing spatially variable soil Young's modulus using spatial average, Struct. Saf. 66 (2017) 106–117, doi:10.1016/j.strusafe.2017.03.001.

[5] C.R. Dietrich, G.N. Newsam, Fast and exact simulation of stationary Gaussian processes through circulant embedding of the covariance matrix, SIAM J. Sci. Comput. 18 (4) (1997) 1088–1107, doi:10.1137/S1064827592240555.

[6] G.A. Fenton, Error evaluation of three random-field generators, J. Eng. Mech. 120 (12) (1994) 2478–2497, doi:10.1061/(ASCE)0733-9399(1994)120:12(2478).

[7] G.A. Fenton, E.H. Vanmarcke, Simulation of random fields via local average subdivision, J. Eng. Mech. 116 (8) (1990) 1733–1749, doi:10.1061/(ASCE)0733-9399(1990)116:8(1733).

[8] G.A. Fenton, D.V. Griffiths, Three-dimensional probabilistic foundation settlement, J. Geotech. Geoenviron. Eng. 131 (2) (2005) 232–239, doi:10.1061/(ASCE)1090-0241(2005)131:2(232).

[9] G.A. Fenton, D.V. Griffiths, Risk Assessment in Geotechnical Engineering, John Wiley & Sons, Hoboken, 2008.

[10] G.A. Fenton, F. Naghibi, M.A. Hicks, Effect of sampling plan and trend removal on residual uncertainty, Georisk 12 (4) (2018) 253–264, doi:10.1080/17499518.2018.1455106.

[11] S. Firouzianbandpey, L.B. Ibsen, D.V. Griffiths, M.J. Vahdatirad, L.V. Andersen, J.D. Sørensen, Effect of spatial correlation length on the interpretation of normalized CPT data using a kriging approach, J. Geotech. Geoenviron. Eng. 141 (12) (2015) 04015052, doi:10.1061/(ASCE)GT.1943-5606.0001358.

[12] R.G. Ghanem, P.D. Spanos, Stochastic Finite Elements: A Spectral Approach (revised edition), Springer-Verlag New York Inc., New York, 1991.

[13] D.V. Griffiths, J. Huang, G.A. Fenton, On the reliability of earth slopes in three dimensions, Proc. R. Soc. A Math. Phys. Eng. Sci. 465 (2110) (2009) 3145–3164, doi:10.1098/rspa.2009.0165.

[14] R.A. Horn, C.R. Johnson, Topics in Matrix Analysis, Cambridge University Press, Cambridge, 1991.

[15] D.T. Hristopulos, Covariance functions motivated by spatial random field models with local interactions, Stoch. Env. Res. Risk. A. 29 (3) (2015) 739–754, doi:10.1007/s00477-014-0933-0.

[16] M.B. Jaksa, J.S. Goldsworthy, G.A. Fenton, W.S. Kaggwa, D.V. Griffiths, Y.L. Kuo, H.G. Poulos, Towards reliable and effective site investigations, Géotechnique 55 (2) (2005) 109–121, doi:10.1680/geot.2005.55.2.109.

[17] S.H. Jiang, J. Huang, F. Huang, J. Yang, C. Yao, C.B. Zhou, Modelling of spatial variability of soil undrained shear strength by conditional random fields for slope reliability analysis, Appl. Math. Model. 63 (2018) 374–389, doi:10.1016/j.apm.2018.06.030.

[18] D.Q. Li, T. Xiao, Z.J. Cao, C.B. Zhou, L.M. Zhang, Enhancement of random finite element method in reliability analysis and risk assessment of soil slopes using Subset Simulation, Landslides 13 (2) (2016) 293–303, doi:10.1007/s10346-015-0569-2.

[19] D.Q. Li, T. Xiao, Z.J. Cao, K.K. Phoon, C.B. Zhou, Efficient and consistent reliability analysis of soil slope stability using both limit equilibrium analysis and finite element analysis, Appl. Math. Model. 40 (9–10) (2016) 5216–5229, doi:10.1016/j.apm.2015.11.044.

[20] Y.J. Li, M.A. Hicks, P.J. Vardon, Uncertainty reduction and sampling efficiency in slope designs using 3D conditional random fields, Comput. Geotech. 79 (2016) 159–172, doi:10.1016/j.compgeo.2016.05.027.

[21] Y. Liu, F.H. Lee, S.T. Quek, M. Beer, Modified linear estimation method for generating multi-dimensional multi-variate Gaussian field in modelling material properties, Probab. Eng. Mech. 38 (2014) 42–53, doi:10.1016/j.probengmech.2014.09.001.

[22] W.F. Liu, Y.F. Leung, Characterising three-dimensional anisotropic spatial correlation of soil properties through in situ test results, Géotechnique 68 (9) (2018) 805–819, doi:10.1680/jgeot.16.P.336.

[23] K.K. Phoon, J.V. Retief, J. Ching, M. Dithinde, T. Schweckendiek, Y. Wang, L.M. Zhang, Some observations on ISO2394: 2015 Annex D (reliability of geotechnical structures), Struct. Saf. 62 (2016) 24–33, doi:10.1016/j.strusafe.2016.05.003.

[24] E. Samaras, M. Shinozuka, A. Tsurui, ARMA representation of random processes, J. Eng. Mech. 111 (3) (1985) 449–461, doi:10.1061/(ASCE)0733-9399(1985)111:3(449).

[25] M. Shinozuka, G. Deodatis, Simulation of multi-dimensional Gaussian stochastic fields by spectral representation, Appl. Mech. Rev. 49 (1) (1996) 29–53, doi:10.1115/1.3101883.

[26] P.D. Spanos, M. Beer, J. Red-Horse, Karhunen–Loève expansion of stochastic processes with a modified exponential covariance kernel, J. Eng. Mech. 133 (7) (2007) 773–779, doi:10.1061/(ASCE)0733-9399(2007)133:7(773).

[27] D. Straub, I. Papaioannou, Bayesian updating with structural reliability methods, J. Eng. Mech. 141 (3) (2015) 04014134, doi:10.1061/(ASCE)EM.1943-7889.0000839.

[28] B. Sudret, A. Der Kiureghian, Stochastic Finite Element Methods and Reliability: a State-Of-The-Art Report, Department of Civil and Environmental Engineering, University of California, Berkeley, 2000.

[29] I.C. Tsantili, D.T. Hristopulos, Karhunen–Loève expansion of spartan spatial random fields, Probab. Eng. Mech. 43 (2016) 132–147, doi:10.1016/j.probengmech.2015.12.002.

[30] E.H. Vanmarcke, Random Fields: Analysis and Synthesis (Revised and Expanded New Edition), World Scientific Publishing Co. Pte. Ltd., Singapore, 2010.

[31] M. Vořechovský, Simulation of simply cross correlated random fields by series expansion methodsg, Struct. Saf. 30 (4) (2008) 337–363, doi:10.1016/j.strusafe.2007.05.002.

[32] Y. Wang, Z. Cao, S.K. Au, Practical reliability analysis of slope stability by advanced Monte Carlo simulations in a spreadsheet, Can. Geotech. J. 48 (1) (2011) 162–172, doi:10.1139/T10-044.

[33] T. Xiao, D.Q. Li, Z.J. Cao, S.K. Au, K.K. Phoon, Three-dimensional slope reliability and risk assessment using auxiliary random finite element method, Comput. Geotech. 79 (2016) 146–158, doi:10.1016/j.compgeo.2016.05.024.
[34] T. Xiao, D.Q. Li, Z.J. Cao, X.S. Tang, Full probabilistic design of slopes in spatially variable soils using simplified reliability analysis method, Georisk 11 (1) (2017) 146–159, doi:10.1080/17499518.2016.1250279.
[35] T. Xiao, D.Q. Li, Z.J. Cao, L.M. Zhang, CPT-based probabilistic characterization of three-dimensional spatial variability using MLE, J. Geotech. Geoenviron. Eng. 144 (5) (2018) 04018023, doi:10.1061/(ASCE)GT.1943-5606.0001875.
[36] T. Zhao, S. Montoya-Noguera, K.K. Phoon, Y. Wang, Interpolating spatially varying soil property values from sparse data for facilitating characteristic value selection, Can. Geotech. J. 55 (2) (2018) 171–181, doi:10.1139/cgj-2017-0219.
[37] Z. Zheng, H. Dai, Simulation of multi-dimensional random fields by Karhunen–Loève expansion, Comput. Methods Appl. Mech. Eng. 324 (2017) 221–247, doi:10.1016/j.cma.2017.05.022.
[38] H. Zhu, L.M. Zhang, T. Xiao, X.Y. Li, Generation of multivariate cross-correlated geotechnical random fields, Comput. Geotech. 86 (2017) 95–107, doi:10.1016/j.compgeo.2017.01.006.